

Chapter 11

**BIRTH, EVOLUTION AND DEATH OF A LAGOON:
LATE PLEISTOCENE TO HOLOCENE
PALAEOENVIRONMENTAL RECONSTRUCTION
OF THE DOÑANA NATIONAL PARK (SW SPAIN)**

***F. Ruiz^{1,*}, M. Pozo², M. I. Carretero³, M. Abad¹,
M. L. González-Regalado¹, J. M. Muñoz⁴, J. Rodríguez-Vidal¹,
L. M. Cáceres¹, J. G. Pendón⁵, M. I. Prudêncio⁶ and M. I. Dias⁶***

¹Departamento de Geodinámica y Paleontología, Universidad de Huelva,
Avda. Tres de Marzo, s/n, 21071-Huelva, Spain

²Departamento de Geología y Geoquímica, Universidad Autónoma de Madrid,
28049-Madrid, Spain

³Departamento de Cristalografía, Mineralogía y Química Agrícola,
Universidad de Sevilla, Apdo. 553, Sevilla, Spain

⁴Departamento de Estadística e Investigación Operativa,
Universidad de Sevilla. 41071- Sevilla, Spain

⁵Departamento de Geología, Universidad de Huelva, Avda.
Tres de Marzo, s/n, 21071-Huelva, Spain

⁶Instituto Tecnológico e Nuclear. EN-10, 2686-953-Sacavém, Portugal

ABSTRACT

A multidisciplinary study of sediment cores from Doñana National Park (SW Spain), a broad region of wetlands in SW Spain, provides the base for the reconstruction of the main palaeoenvironmental changes that occurred in the Guadalquivir estuary since OIS 3. The facies analysis differentiates six main facies, deposited in freshwater pond and marsh (FA-1: laminated silt), brackish marsh or the periphery of a brackish lagoon (FA-2: greyish silt), a shallow lagoon (FA-3: green silt and clay), the marine connection of this

* Corresponding author: Email: ruizmu@uhu.es

lagoon (FA-4: yellow silt) or sandy spit (FA-6: yellow sand), whereas FA-5 includes bioclastic silt and sand with a tsunamigenic origin.

The vertical arrangement of these facies, their dates and a detailed comparison with previous works permit to delimitate ten phases in the Late Pleistocene to Holocene evolution of this lowland. In the oldest phase (OIS 3), this area was occupied by freshwater marshes. Phase 2 (OIS 2) was characterized by the alternation of freshwater and brackish marshes, partly enclosed by aeolian units. During the third phase (Early Holocene), the brackish marshes constituted the northern limit of a broad lagoon that extended along the present-day inner shelf. The sea-level highstand of the Present Interglacial (Flandrian transgression, phase 4: ~6.5 cal BP) caused the inundation of this area, occupied by an open lagoon. Between 6.5 and 4.6 cal ka (phase 5), incipient brackish marshes emerged along the margins of this lagoon and a first tsunamigenic event (5100-4800 cal BP) eroded partially the Doñana spit. The following phase (4.6-3.7 cal ka) was relatively quiet, with predominance of infilling processes. This calm scenario was interrupted by a new period of instability (phase 7: 3.7-3 cal ka), with two new high-energy events. The progressive infilling is the main feature of phase 8 (3-2.2 cal ka), with the emersion of new brackish marshes and a decreasing depth in the adjacent lagoon. The first historical tsunamis (phase 9: 2.2-1.9 cal ka) induced the creation of washover fans and bioclastic ridges overlying the previous marshes. Since 1.9 cal ka (phase 10), the growing of the Doñana spit and the fluvial-tidal sediment inputs caused an important filling of the Guadalquivir estuary (Doñana National Park), only interrupted by new tsunami records (~1.8-1.5 cal ka).

1. INTRODUCTION

The Pleistocene-Holocene geological record of littoral areas has received an increasing attention in the last decades. The multidisciplinary analysis of cores collected in lagoons, estuaries, salt marshes or deltas has revealed a broad information about the palaeoenvironmental evolution of these environments, global or regional sea-level changes, palaeoclimatology or the effects of anthropogenic actions during this period (Borrego et al., 2004; Vilanova et al., 2006; Selby and Smith, 2007). In this scenario, the mineralogical composition plays is an important tool to infer the origin of sediments, the variations of some physical-chemical water parameters or even palaeoclimatic oscillations (Chamley, 1989; Carretero et al., 2002; Mackie et al., 2007).

This record includes distinctive sedimentary layers that have been attributed to storms, cyclones, hurricanes or tsunamis. These high-energy events cause the deposition of sedimentary layers with characteristic textural and mineralogical features (Clague et al., 2000; Singarasubramanian et al., 2006; Babu et al., 2007). In most cases, these investigations are concentrated on a single event (Dawson and Smith, 2000; Wagner et al., 2007), although even six tsunamis have been recognized in a single section (e.g., Cisternas et al., 2005).

The southwestern Spanish coast is a low-probability tsunamigenic area (Galbis, 1932, Campos, 1991; Reicherter, 2001), with sixteen documented tsunamis between 218 BC and 1900 AC. Nevertheless, its geological record is poorly known at present (e.g., Luque et al., 2001; 2002; Ruiz et al., 2004; 2005a; Scheffers and Kelletat, 2005).

The aim of this chapter is to delimitate the main sedimentary facies deposited in the Doñana National Park (SW Spain) during the Late Pleistocene-Late Holocene period, with special attention to their textural, mineralogical and palaeontological features. Its vertical and

lateral dispositions, together with radiometric datings, will permit to reconstruct the palaeoenvironmental evolution of this area in relation with climatic changes and sea level oscillations.

2. STUDY AREA

The Doñana National Park (SW Spain) is located on the western bank of the Guadalquivir estuary, with an extension of 50,720 ha (Figure 1). This area constitutes one of the largest wetlands in Europe, composed mainly of salt and freshwater marshes that include temporary ponds and have a modest topographic gradient (0-1 m). These marshes are drained by two main tributaries (Guadimar River and Madre de las Marismas Creek) and numerous ebb-tide channels, with recent and former banks occupied by clayey levees and both bioclastic and beach-morphology ridges (Figure 1: Veta la Arena, Las Nuevas). In addition, they are locally covered by sandy ridges located very close to the Doñana spit and disposed in a NE-SW direction (Figure 1: Carrizosa, Vetallengua).

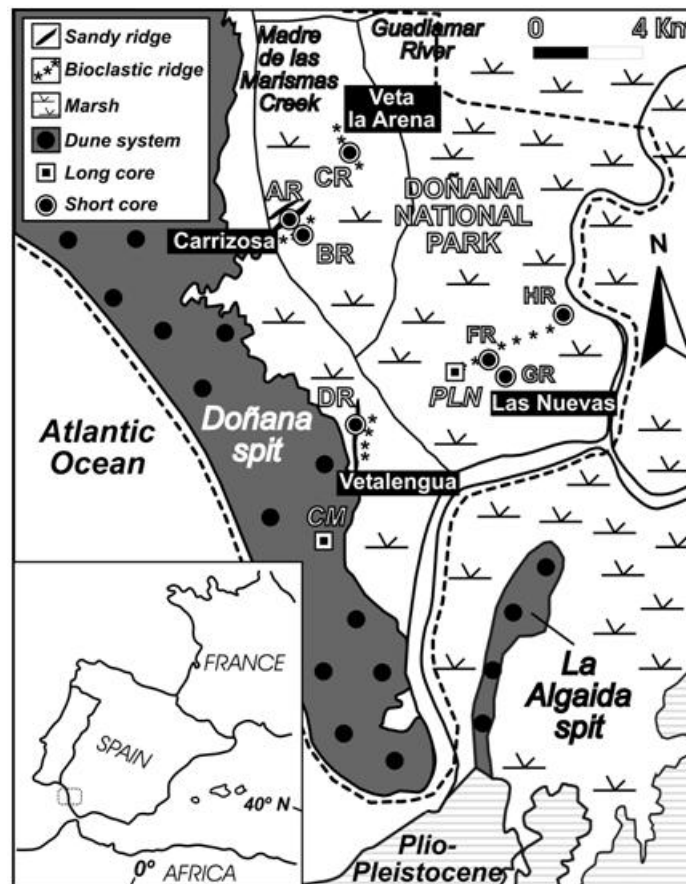


Figure 1. Geographical setting and geomorphology of the Doñana National Park, with location of the cores

These inner zones are partly protected by two sandy spits (Doñana and Algaida; 0-30 m height). They include active dune systems disposed in narrow (< 100 m) and elongated (1–2 km) alignments.

The main hydrodynamic processes are controlled by the fluvial regime, tidal inputs, the southwestern dominant wave action and the southeastern drift currents. The Guadalquivir River has a very irregular regime, with an annual mean of $185 \text{ m}^3 \text{ s}^{-1}$ and a maximum up to $1000 \text{ m}^3 \text{ h}^{-1}$ (Vanney, 1970; Menanteau, 1979). The tidal regime is mesotidal and semidiurnal, with an average tidal range of approximately 3.6 m (Borrego et al., 1993).

3. MATERIALS AND METHODS

3.1. Textural, Mineralogical and Paleontological Analyses

Two long cores (Figure 1: *PLN* -93 m-; *CM* -31 m-) were collected by the Spanish Geological and Mining Institute (IGME) in the southern part of the Doñana National Park. Additional samples were obtained from seven short cores included by Ruiz et al. (2004; 2005a) in previous works. The main facies were established from lithological descriptions complemented with the grain-size analysis of seventy representative samples, owing the predominance of detrital facies (Figures 2-3-4). Grain-size distribution was determined by dry sieving for the coarser fractions. Fractions lesser than $100 \mu\text{m}$ were analysed by photosedimentation (MicromeriticsR Sedigraph 5100 ET) using Na-hexametaphosphate as a dispersing agent.

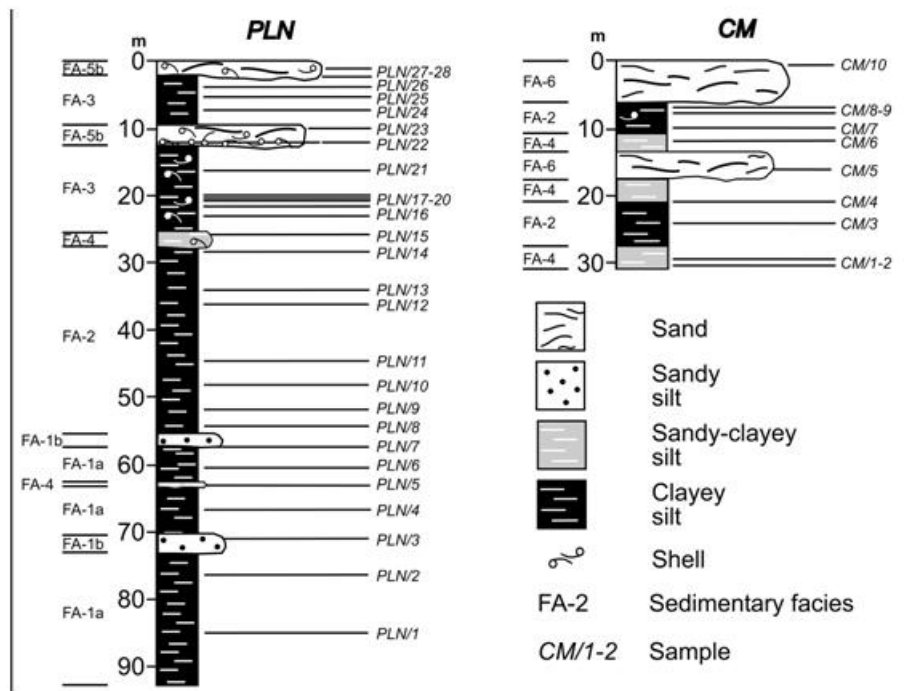


Figure 2. Long cores. Distribution of facies and mineralogical samples

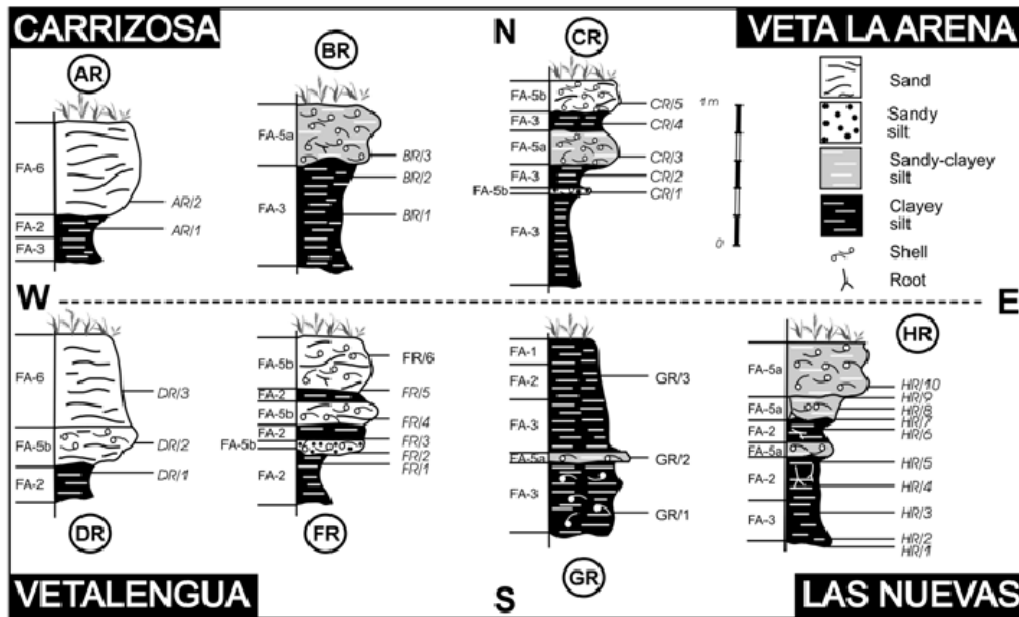


Figure 3. Short cores. Distribution of facies and mineralogical samples

The mineralogical analysis of samples was carried out by means of X-ray diffraction (XRD) using a Siemens D-5000 equipment with a scanning speed of $1^{\circ}2\theta/\text{min}$ and $\text{Cu-K}\alpha$ radiation. XRD studies were performed both on randomly oriented samples (total fraction) and clay fraction samples ($< 2 \mu\text{m}$), the last prepared from cation-saturated, ultrasonic treated suspensions oriented on glass slides. The identification of the clay fraction minerals was carried out on oriented Mg^{2+} -saturated samples with ethylene glycol salvation, and also after heating at 550°C following K^{+} saturation. When required, carbonates were eliminated using 0.6 N acetic acid.

Quantitative estimation of the mineral content was carried out using the intensity factors calculated by Schultz (1964) and Barahona (1974). Results from 65 bulk samples and 41 oriented clay samples are shown in Tables 1 and 2, respectively.

In addition, the $>63 \mu\text{m}$ fraction was revised under stereoscopic microscope, in order to effectuate a general revision of the palaeontological record. This revision includes the taxonomical determination and the estimation of both densities and diversities of bivalves, gastropods, ostracods and foraminiferids. In addition, the presence and relative abundance of other groups (scaphopods, barnacles, bryozoans, crabs) have been also detailed.

3.2. Mathematical Procedures

A multivariate analysis was applied to determine the mineralogical sample groups based on the percentages computed of the main minerals (quartz, calcite, phyllosilicates, feldspars and dolomite). An initial clustering procedure is applied using a hierarchical agglomerative technique with the application of the Euclidean distance and the Ward linkage. Results are contrasted by discriminant analysis, by determining both the dimensions and variables on

which the groups differ. In addition, a stepwise selection procedure was computed and the contribution of each of the predictor variables to the overall discrimination was determined. The error rate estimation was obtained by a final cross-validation method. These statistical techniques were carried out using several subprograms of the Statistical Package for the Social Sciences (SPSS™). Further details of these techniques may be consulted in Dillon and Goldstein (1984).

3.3. Radiocarbon Chronology

Two new dates were produced at the Beta Analytic Laboratory (Miami, USA) by radiocarbon analysis of mollusc shell (Figure 6. core CM), whereas the remaining twelve dates were obtained from Ruiz et al. (2004; 2005 a, b) and Pozo et al. (in press). All data were calibrated using CALIB version 5.0.2 (Stuiver and Reimer, 1993) and the Stuiver et al. (1998) calibration dataset. The final results correspond to calibrated ages (ca.) using 2σ intervals, with the reservoir corrections suggested by Soares and Dias (2006 a, b) and Soares (2008) for this area. For the time interval 4500-4000 yr BP, more future results are necessary to determine a mean value to be used with the marine calibration curve (Soares, personal communication). Ages discussed below are expressed as the highest probable age of the 2σ calibrated range (e.g., Van der Kaars et al., 2001).

In addition, the calibrated age of the maximum of the Flandrian transgression has been used (Zazo et al., 1994; Figure 6: **) and the sedimentation rates (1.5-2.5 mm/yr) deduced from Spanish Holocene estuarine sequences (Lario et al., 2002; Zazo et al., 2008) for the interval 10,000-7000 yr BP have been applied to core PLN (see Figure 6: ***)

3.4. Palaeogeographical Reconstruction

The palaeogeographical evolution of this area has been possible with: a) the inclusion of numerous data obtained by Lario (1996), Zazo et al. (1999) and Yll et al. (2003) in other cores of the Doñana National Park; b) the analysis of several boreholes drilled near the Guadiamar River mouth by Salvany et al. (2001); c) the palaeogeographical interpretation of numerous seismic profiles effectuated in the Cádiz Gulf (Lobo et al., 2001; 2002); and d) previous analyses of short cores (Figure 3) by Ruiz et al. (2004; 2005a).

4. RESULTS AND DISCUSSION

4.1. Facies and Palaeoenvironmental Interpretation

Six main facies have been differentiated:

Facies FA-1. Laminated silt. This facies occupies the lowest 30 m of core PLN and the upper 32 cm of core GR. It consists mainly of clayey silt (Figure 2: Facies FA-1-a), with up to 65 % of sediments included in the $40\ \mu\text{m}$ - $4\ \mu\text{m}$ grain size interval. These sediments show a

fine parallel lamination, with alternation of greyish to greenish (colour 6/1; Munsell scale) and blackish (colour 4/1) layers. Some layers of sandy-clayey silt (Facies FA-1-b: sand ~10-15 %) are also interbedded within this general pattern. Phyllosilicates (42-73 %) are clearly dominant over calcite (11-21%), quartz (8-13 %) and feldspars (2-27 %) in the clayey-silty layers, whereas quartz increases remarkably (20-40%) in the sandier laminae. The clay mineral contents are very variable (smectites: 25-56 %; illite: 25-56 %; kaolinite: 4-27 %).

The microscopical analysis reveals the presence of numerous reddish, oxidized fragments of roots and phanerogams, scarce gyrogonites of characeans (*Chara* sp., *Nitella* sp.) and isolated fragments of undifferentiated bivalves. A freshwater ostracod assemblage (*Cyprinotus salinus*, *Cyprideis torosa*, *Ilyocypris gibba*, *Cyprideis torosa*, *Herpetocypris chevreuxi*, *Cypris bispinosa*) is very abundant in core GR, whereas only scarce specimens of the two first species have been found in core PLN.

Interpretation. The main features of Facies FA-1-a have been observed in temporary ponds and the surrounding freshwater marshes of the Doñana National Park, with similar ostracod and characean assemblages (Ruiz et al., 1996; Santos et al., 2006). These ponds are very shallow (< 1 m in most cases) and contain alkaline, fresh to oligohaline waters (Serrano and Toja, 1995). Fine laminations will indicate a calm environment with a cyclic sedimentation suggested by the alternating color shades, probably due to alternating dry or wet periods, pulses from small tributaries or the vegetation distribution (Whittecar et al., 2001; Harter and Mitsch, 2003). The almost absence of microfauna in the oldest sediments may be due to the dissolution of the thin carapaces of the freshwater species (e.g., ostracods), a process very usual in similar (paleo-)environments during the oxidation of organic matter (Hoge, 1994; Smith, 1997). The higher grain size of Facies FA-1-b and the absence of faunal remains are attributed to increasing fluvial inputs.

Facies FA-2. Greyish silt. This facies is widely represented in almost all cores and is constituted by silt and clay (silt: 55-70 %; clay: 26-43 %) with greyish to greenish colours (colour 5Y 4/2). Up to 70 % of sediment is comprised between 15 and 2 μm (Figure 4), with high percentages of fine and very fine silt. They are massive or show a very tenuous lamination. Phyllosilicates are the main mineral components (24-73 %; mean 48 %), although both quartz (8-34 %; mean 14 %) and calcite (8-35 %; mean 23.3 %) increase in relation to FA-1. Smectites (> 44 % in most cases) are dominant over illite (mean: 37.2%) and kaolinite (11.7 %).

The palaeontological record includes low densities of a high brackish ostracod assemblage (mainly *C. torosa*, *Loxoconcha elliptica*, *Leptocythere castanea*), salt marsh foraminifers (*Ammonia tepida*, *Jadammina macrescens*, *Haynesina germanica*, *Trochammina inflata*), scarce pulmonate gastropods and undifferentiated fragments of stems and roots. Reworked specimens of planktonic foraminifers, spines of echinoderms, bryozoans and marine or brackish bivalves (*Cardium edule*, *Venerupis decussatus*) are frequent.

Interpretation. This facies has intermediate characteristics between FA-1 and FA-3. The microfossil assemblages are characteristic of brackish marsh or the surrounding margins of a brackish lagoon. Tidal flows introduced marine faunas toward the more protected areas of this lagoon. Both mineralogical and palaeontological records are very similar to those observed in

the inner areas of perimediterranean lagoons (Carbonel and Pujos, 1982; Montenegro and Pugliese, 1996; Ruiz et al., 2006b).

Facies FA-3. Green silt and clay. It consists of greenish clayey silt or silty clay (colour 10YR 5/3), with up to 70 % of sediment (dry weight) comprised between 30 μm and 1 μm and very low sand contents (< 4 %). This facies exhibits a fine parallel lamination, with coarse laminae (5-10 cm thick) well defined and scarce evidence of bioturbation.

The bulk mineralogy is dominated by phyllosilicates (32-62 %), reaching usually up to 41 %. Calcite (19-32 %; mean 24 %) and quartz (10-23 %; mean 15.5 %) have more homogeneous distributions than FA-2, although similar mean values. The highest contents of feldspars (1-15 %) and dolomite (2-17 %) were found in core PLN (20-25 m depth).

Clay minerals show an interesting contrast between core PLN and the remaining ones. In the upper part of this core, illite is clearly dominant (48-53 %) over smectites (26-32 %), whereas these latter are more abundant (51-67 %) in the inner cores or near the protected, landward side of the Doñana spit.

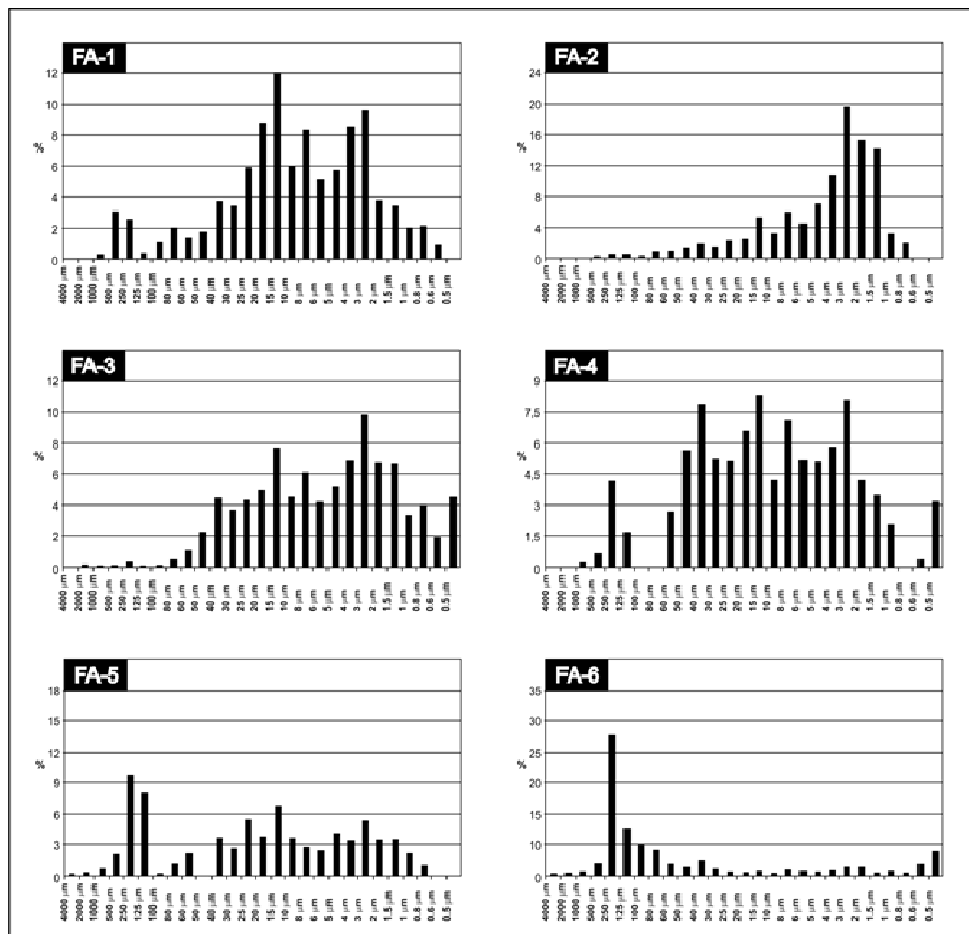


Figure 4. Photosedimentation grain-size analyses of the six facies differentiated, expressed as mean percentages of each grain size interval in each facies. See differences between subspecies in the text

Table 1. Bulk mineralogy of selected samples

SAMPLES	Quartz	Calcite	Phyllosilicates	Feldspars	Dolomite	Others
CM-9	10	22	62	3	3	0
CM-8	27	24	40	3	3	3
CM-6	44	20	15	19	2	0
CM-5	71	4	3	21	1	0
CM-3	13	23	56	2	6	0
PLN-28	13	28	42	7	7	3
PLN-27	14	31	33	8	11	3
PLN-26	10	19	54	3	9	5
PLN-25	16	26	45	4	2	7
PLN-24	14	28	43	4	8	3
PLN-23	10	22	34	24	9	1
PLN-22	12	12	35	13	24	4
PLN-21	16	21	51	7	5	0
PLN-20	14	28	44	5	6	3
PLN-19	20	20	55	2	3	0
PLN-18	14	31	32	5	17	1
PLN-17	13	24	41	15	5	2
PLN-16	18	24	33	8	14	3
PLN-15	20	32	35	6	7	0
PLN-14	12	33	45	4	6	0
PLN-13	8	23	61	3	5	0
PLN-12	7	31	49	5	6	2
PLN-11	14	34	32	8	12	0
PLN-10	17	28	31	14	8	2
PLN-9	14	21	24	8	32	1
PLN-8	9	27	44	8	12	0
PLN-7	34	8	24	23	11	0
PLN-6	8	18	67	5	2	0
PLN-5	14	16	47	5	18	0
PLN-4	11	11	48	27	3	0
PLN-3	39	15	28	13	5	0
PLN-2	12	21	52	11	4	0
PLN-1	13	32	42	4	9	0
AR2	62	2	30	5	1	0
AR1	13	15	43	2	2	25 (Gypsum)
BR3	4	40	56	0	0	0
BR2	16	21	54	3	4	2
BR1	11	20	62	0	2	5
CR5	75	21	3	1	0	0
CR4	23	24	46	3	4	0
CR3	17	34	43	1	4	1

Table 1. (Continued)

SAMPLES	Quartz	Calcite	Phyllosilicates	Feldspars	Dolomite	Others
CR2	20	23	53	2	2	0
CR1	41	35	20	2	2	0
DR3	88	1	6	5	0	0
DR2	75	2	11	10	1	1
DR1	12	16	67	1	4	0
FR6	42	25	13	8	12	0
FR5	45	21	10	8	16	0
FR4	37	30	12	13	8	0
FR3	14	35	44	4	3	0
FR2	36	22	31	4	7	0
FR1	18	20	53	4	5	0
GR3	8	14	73	3	2	0
GR2	11	20	61	3	5	0
GR1	13	21	58	3	4	1
HR10	18	21	53	3	3	2
HR9	10	19	60	5	3	3
HR8	9	21	61	2	3	4
HR7	9	20	65	2	2	2
HR6	11	21	61	2	3	2
HR5	10	24	58	4	2	2
HR4	12	25	55	4	2	2
HR3	13	32	47	1	3	4
HR2	16	27	49	2	3	3
HR1	16	19	51	9	3	2

Macrofauna is composed of brackish (mainly *Cardium edule*) and marine (*Venerupis decussatus*, *Chamelea gallina*) bivalves, together with less frequent specimens of marine gastropods (*Rissoa*, *Hinia*). Ostracods (2-200 individuals/gram; *C. torosa*, *L. elliptica*, *L. castanea*) and foraminifers (10-1,000 individuals/gram; *A. tepida*, *H. germanica*) are frequent to very abundant in these sediments. The reworked marine faunas of ostracodes, planktonic foraminifers, spines of echinoderms, fragments of bryozoans or central diatoms may be locally abundant, composing 20-40 % of the paleontological record.

Interpretation. The most representative species of both ostracodes and foraminifers are well represented in the deeper, subtidal areas of brackish lagoons (salinity up to 15-20 ‰), located near a river mouth. In these coastal areas, the tidal renewal is conditioned by the dimensions of outlets that cross the external, elongated sandy spits (Marocco et al., 1996; Samir, 2000; Ruiz et al., 2006a). This marine influence is contrasted by the presence of reworked faunas derived from the adjacent infralittoral zone (Pérez Quintero, 1989; Ruiz et al., 1997). The different clay mineralogy may be explained by the more open location of core PLN within this lagoon, with inputs of illite-rich, silty-clayey sediments from the shelf. In these shallow marine areas of southwestern Spain, illite is dominant over smectites (Gutiérrez-Mas et al., 1997).

Table 2. Clay mineralogy of selected samples

SAMPLES	Smectites	Illite	Kaolinite
CM-9	45	38	17
CM-3	46	42	12
PLN-26	30	51	19
PLN-25	26	53	21
PLN-21	32	48	20
PLN-17	31	49	20
PLN-14	38	39	23
PLN-12	58	31	11
PLN-11	44	41	15
PLN-6	31	46	23
PLN-4	56	25	19
PLN-2	25	56	19
PLN-1	47	42	11
AR2	67	31	2
AR1	54	40	6
BR3	41	52	7
BR1	67	29	4
CR5	35	59	6
CR4	50	37	13
CR3	46	50	4
CR2	56	35	9
CR1	52	39	9
DR3	61	37	2
DR2	29	59	12
DR1	56	34	10
FR6	26	60	5
FR4	35	54	11
FR1	49	39	12
GR3	41	51	8
GR2	28	68	4
GR1	53	40	7
HR10	47	43	10
HR9	42	50	8
HR8	34	57	9
HR7	43	49	8
HR6	57	33	10
HR5	60	33	7
HR4	55	36	9
HR3	57	37	6
HR2	51	41	8
HR1	58	36	6

Facies FA-4. Yellow silt. It is constituted by off-white to pale yellow, sandy-clayey silt (colour 8/2 to 8/3), poorly sorted, with very low to moderate percentages of sand (4-20 %). They present a very tenuous low-angle cross stratification, parallel lamination or absence of patent sedimentary structures.

These fine-grained sediments are characterized by moderate to high percentages of quartz (20-44 %) and low to moderate phyllosilicate contents (15-35 %). In addition, calcite exceeds 20 % and feldspars can be significant (~ 20 %) in the upper part of core CM. Smectites and illite show similar proportions (40-50 %).

Macrofauna is abundant, with numerous valves and fragments of marine molluscs, including bivalves (*C. gallina*, *V. decussatus*, *Acanthocardia tuberculata*), gastropods (*Rissoa* spp., *Hinia reticulata*, *Lemintina arenaria*) and scaphopods (*Dentalium vulgare*, *D. sexangulum*). Benthic marine foraminifers (50-300 individuals/gram; *Ammonia beccarii*, *Quiqueloculina* spp., *Elphidium crispum*) and ostracodes (*Palmoconcha turbida*, *Pontocythere elongata*, *Urocythereis oblonga*) are dominant over brackish species. Fragments of bryozoans, plates of barnacles, claws of crabs, or planktonic foraminifers (*Orbulina*, *Globigerina*, *Globigerinoides*) are also abundant.

Interpretation. The most abundant assemblages of molluscs, ostracodes and foraminifers of this facies characterize the shallow areas (< 40 m depth) of the southwestern Spanish shelf (Pérez Quintero, 1989; Ruiz et al., 1997; González-Regalado et al., 2000). These assemblages and some brackish specimens (*C. torosa*, *L. castanea*) are usually found in the marine zones of perimediterranean lagoons, very close to the natural or artificial inlets and subjected to moderate to high hydrodynamic gradients (Ruiz et al., 2000; 2006, a; b).

Facies FA-5. Bioclastic silt and sand. This facies is the main constituent of several bioclastic ridges located in the margins of recent or former tidal channels (Figure 1: Veta la Arena, Las Nuevas). These sedimentary beds are characterized by a large lateral extension (3-6 km) and a narrow width (20-30 m). Thickness (5-70 cm in most cases) decreases landward, being disposed usually over FA-2 or FA-3. They display an erosive base, with vegetation remains and intraclasts of the underlying sediments in the lower centimetres. In the upper part, bioclasts were disposed in thick laminae (3-5 cm) or present a disorganized disposition, being fragmented in most cases.

Texture permits to delimitate two subfacies, with a bimodal grain size distribution and a poor sorting in both cases:

Subfacies FA-5-a. Bioclasts are included in a greenish, clayey-silty matrix (colour 5Y 8/3), with moderate sand contents (10-25 %). Phyllosilicates (43-65 %) are clearly dominant over calcite (19-40 %) and quartz (4-18 %). Illite is the main clay mineral (43-68%), with percentages slightly higher than smectites (28-47 %). This subfacies is dominant in Veta la Arena and the northeastern part of Las Nuevas.

Subfacies FA-5-b. It is represented in the cores located near the Doñana spit. This subfacies will be transitional to FA-6, with bioclasts included in a greenish to greyish silty-sandy matrix (colour 5Y 8/6). The mineralogical composition is very variable, ranking from quartz-rich samples (quartz up to 70 %) to others dominated by phyllosilicates (30-40 %) and calcite (12-31 %). Dolomite can be occasionally important (10-24 %). Illite ranges between 50% and 60% in all samples. This subfacies is well represented in Vetallengua and the southwestern part of Las Nuevas. In this last ridge, grain size seems diminish landward and easternward. In general, these ridges fines upward, passing from basal fine sands to very fine sands with important silty percentages near the top.

Molluscs represent an important proportion (10-40 % dry weight) of the sediment. Shell debris and disarticulated bivalve shells of estuarine (mainly *Cardium edule*) and marine (mainly *Acanthocardia tuberculata*, *Donax vittatus* and *Spisula solida*) are abundant. Gastropods are represented by freshwater (*Gyraulus laevis*, *Melanopsis*) and marine (*Rissoa*, *Lemintina*, *Hinia*) specimens. Fragments of barnacles, scaphopods and bryozoans are also frequent.

Microfauna is better represented in subfacies FA-5-a, with 50-500 individuals/gram of brackish ostracodes (*C. torosa*, *L. elliptica*) and foraminifers (*A. tepida*, *H. germanica*), together with marine specimens of both groups (*Basslerites berchoni*, *Carinocythereis whitei*, *Urocythereis britannica*, *Ammonia beccarii*, *Elphidium crispum*). Some marine miliolids are also abundant (*Triloculina*, *Quinqueloculina*), with a frequent loss or rupture of the last chambers. Brackish ostracodes present a high-energy population structure, with numerous individuals (>70 % in most of samples) belonging to adults or A-1 to A-3 moults. Only scarce specimens of brackish species were observed in the sandier samples of subfacies FA-5-b.

Interpretation. These ridges show numerous features that have been described in tsunamigenic deposits (Bryant et al., 1992; Bryant, 2001; Costa et al., 2004; Dawson and Steward, 2007): a) an erosional base; b) presence of intraclasts plant remains near the base; c) finer sediments toward the top; d) finer sediments landward; e) presence of higher sand percentages (near the Doñana spit) in relation to the underlying sediments; f) changes in the clay mineral composition, with a general dominance of illite, probably derived from the adjacent shelf where this clay mineral is dominant (Gutiérrez-Más et al., 1997); g) strong changes of fauna in relation to the underlying layers; h) presence of numerous marine species of both macrofauna and microfauna with evidence of reworking; or i) high-energy population structures on ostracodes. Consequently, a tsunamigenic origin has been attributed to these beds.

Facies FA-6. Yellow sand. This facies is represented in the uppermost part of the sandy ridges (Carrizosa, Vetalegua) and the dune system of the Doñana spit (core CM). These layers consists of well sorted, fine to very fine sand with intense yellow shades (colour 10Y 8/6). Up to 60 % of sediment presents a grain size comprised between 500 μm and 80 μm . In the upper levels of core CM, this facies exhibits cross stratification, whereas sand is massive in cores AR and DR. Quartz (62-88 %) is dominant over phyllosilicates (3-30 %) and feldspars (5-21 %). Smectites (54-56 %) are the main clay minerals, with minor proportions of illite (34-40 %) and kaolinite (6-10 %).

Both macrofauna and microfauna are virtually absent, with exception of some isolated and fragmented remains of the bivalve *Corbula gibba*.

Interpretation. These sediments constitute the dune systems of the Doñana spit. The mineralogical records obtained coincide with those indicated by Flor (1990) and the Spanish Environmental Ministry (2005) in these aeolian beds.

The sandy ridges of Carrizosa and Vetalegua show the same textural, mineralogical and faunal features. They occupy the margins of former meanders within the old lagoon system and are disposed at high angles in relation to the Doñana spit. The contact with this sandy bed coincides with the presence of an erosive surface within the dune systems of the spit (Rodríguez Ramírez et al., 1995) and a remarkable slimming of its width.

The presence of these sand layers over FA-2 or FA-3 may be indicative of old tsunamis, with a partial rupture or erosion of the spit and the deposit of washover fans in its inner side. In a second episode, these washover fans would be reworked by the tidal fluxes and deposited in the margins of old tidal channels, constituting the sandy ridges of Carrizosa and Vetallengua. Simultaneously or in a later stage, a part of these washover fans would be dismantled and their almost azoic sands were introduced toward the inner areas of the lagoon, being deposited (as FA-5-b) over fluvial levees or marshes. The vertical facies disposition of core DR, with basal bioclastic layers below sandy beds, is very similar to that indicated in some washover fans of the southwestern Spanish coast and southeastern Asia, derived from recent and past tsunamis (Luque, 2002; Hori et al., 2007).

4.2. Statistical Analysis

4.2.1. Cluster groups

Cluster analysis permits to separate two main groups (Figure 5, A). Group 1 (52 samples) is characterized by high percentages of phyllosilicates (mean 49.1 %) and calcite (> 23 % in most cases). A more detailed analysis defines three subgroups, with very high phyllosilicate contents (Subgroup 1.1), high to very high percentages of both feldspars and dolomite (Subgroup 1.2) and the highest mean percentages of calcite of all groups or subgroups (Subgroup 1.3). The clay mineral pattern of the two first subgroups is unclear, with variable percentages of smectites (25-67 %) and illite (25-68 %). Smectites are generally dominant over illite or both present similar contents in the third subgroup.

Samples (13) of Group 2 consist mainly of quartz (mean 53 %), with phyllosilicates and calcite as secondary constituents. The quartz contents differentiate clearly two subgroups (Subgroup 2.1: mean ~ 40 %; Subgroup 2.2: mean ~ 74 %). Illite is dominant in subgroup 2.1, whereas subgroup 2.2 can be divided between azoic (Figure 5: 2.2.A: smectites: 61-67 %; illite: 31-37%) and bioclastic (2.2.B: smectites: 29-35%; illite ~ 59 %) layers.

4.2.2. Cross-validation

In this final step, all samples are included in the same initial cluster, indicating a true separation between the two groups differentiated. In addition, 59 samples (up to 90 %) were included in the same subgroup, whereas the remaining six were relocated in a different subgroup within Group 1 and no changes were observed in Group 2.

4.2.3. Mineralogical groups vs sedimentary facies

A comparison between these two variables permits to observe some remarkable coincidences (Figure 5, B). The 'inner' facies of this coastal palaeoenvironment (FA-1a: freshwater marsh and pond; FA-2: lagoon margin and brackish marsh; FA-3: subtidal lagoon; FA-5a: tsunamigenic, inner layers) are included in Group 1, whereas those related with 'external' inputs (FA-1-b: fluvial; FA-4: marine; FA-5-b: tsunamigenic, externe aeolian layers; and FA-6: aeolian) are more closely related with Group 2. The presence of some samples belonging to FA-5-b within Group 1 would be explained by the palaeotopography of the lagoon bottom, probably deeper in the central zone (upper part of core PLN).

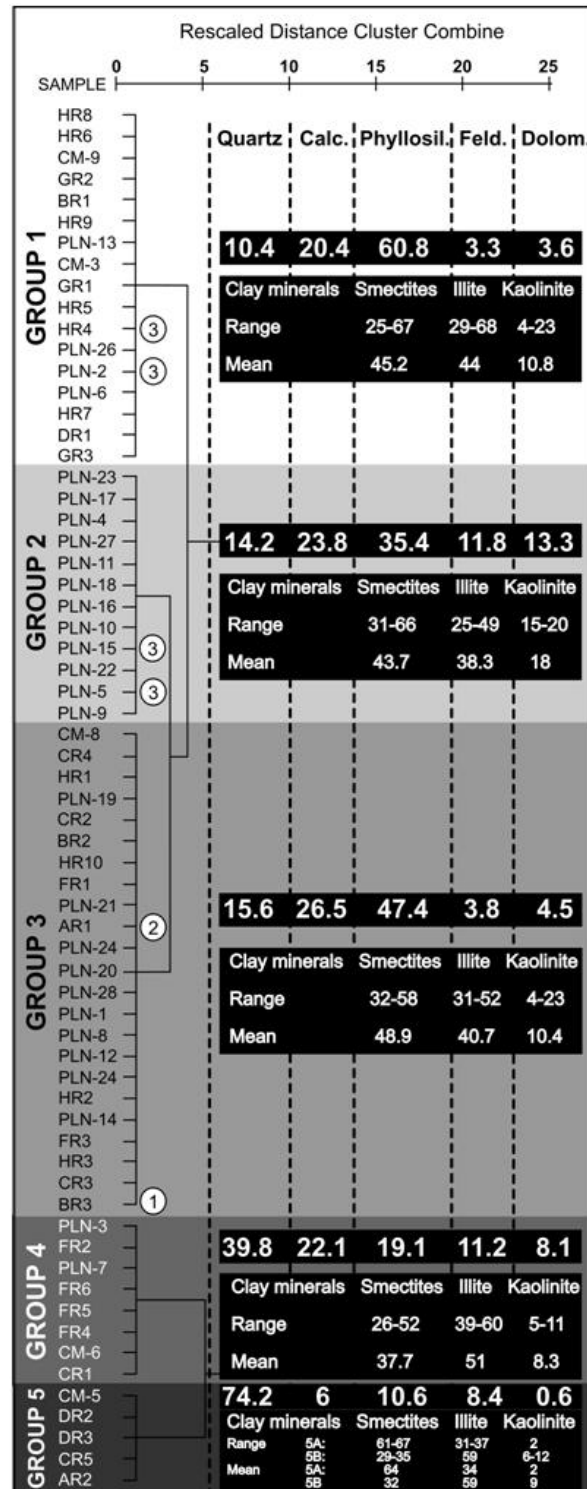


Figure 5. A: Cluster analysis of the mineralogical data, B: Comparison between the mineralogical groups and the sedimentary facies

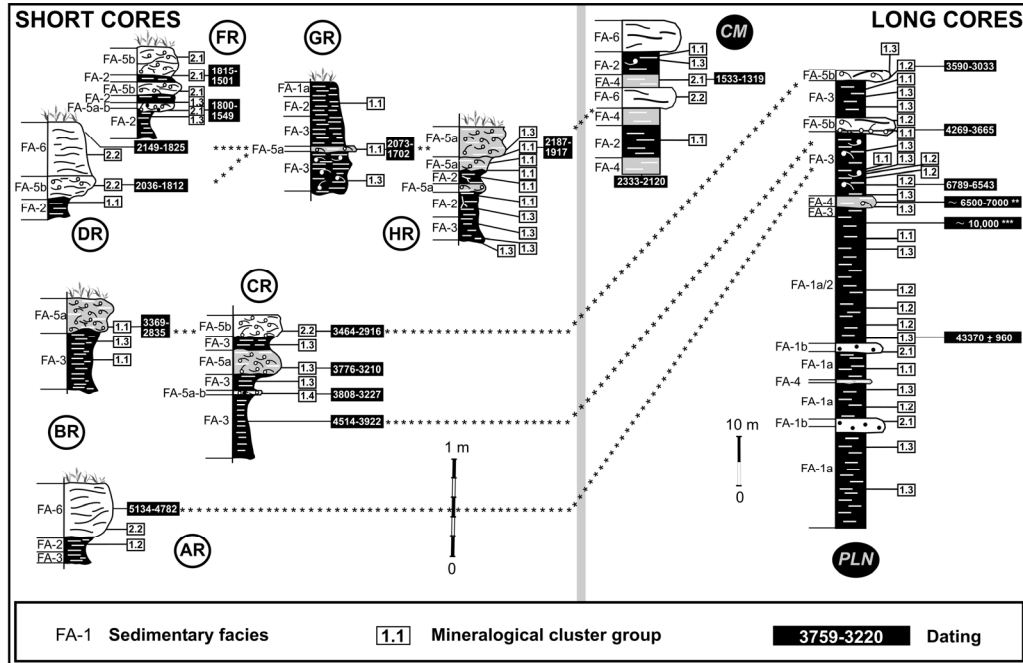


Figure 6. Correlation of the cores, with inclusion of the vertical disposition of facies, the mineralogical groups and datings

4.3. Radiocarbon Datings

The total dataset has seventeen datings, with calibrated ages ranking from ~44 ka to 1.4 ka (Figure 6). Additional data have been inferred in core PLN from: a) the lateral correlation with the adjacent, bioclastic ridge of Las Nuevas (Figure 6: *); b) the maximum of the Holocene transgression in this area (Figure 6: **) inferred by Zazo et al. (1994) and Lario et al. (1995); and c) the general sedimentation ratios (1.5-2.5 mm/yr) deduced between 7000 and 10,000 cal BP interval (Figure 6: ***) in different estuaries of the southern Spanish coast (Lario et al., 2002; Zazo et al., 2008).

5. LATE PLEISTOCENE-LATE HOLOCENE EVOLUTION OF THE DOÑANA NATIONAL PARK

The comparison of these data with others obtained by different investigation teams in the Doñana National Park and the adjacent areas permits to draw a tentative palaeogeographical evolution of this zone. Ten phases may be delimited:

Phase 1 (OIS 3)

Freshwater marsh (Facies FA-1) characterized the easternmost, inner areas of the Doñana National Park during OIS 3 (Figure 7, a-b), with an increasing hydric availability and a moister climate in relation to OIS 4 (Yll et al., 2003; Zazo et al., 2005). This general scenario is only interrupted by a marine input (> 45 ka) that inundated the inner areas and caused the deposition of Facies FA-4 in core PLN. This event may be related to short-lived warmer episodes of interstadial character (Behre, 1989), ice retreat phases (Duplessy et al., 1988), the final phase of a warm period in southern Europe (Van Andel, 2003), a sea level rise (Yokoyama et al., 2001) or a high-energy event. In the western sector, different aeolian units (~ FA-6) were deposited in the El Abalarío area (Zazo et al., 2005).

Sea level oscillated between -80 m and -100 m during this period (Siddall et al., 2003). Consequently, the larger part of the adjacent shelf was exposed, with coastal deposits located in the central area of the Cádiz Gulf (Lobo et al., 2002).

5.2. Phase 2 (OIS 2)

During the Last Glacial Maximum (Figure 7, c), the eastern part of the Doñana National Park was occupied by alternating freshwater and brackish marshes (FA-1a and FA-2). These inner areas are partly enclosed by aeolian units (Zazo et al., 2005).

This phase coincides with the lowest sea level (~ -125 m to -130 m) of the last 100,000 years (Yokoyama et al., 2000). Consequently, the palaeocoastline was located at ~ 40 km to the southwestern of its present-day position (Lobo et al., 2001).

Phase 3 (Early Holocene)

Sea level reached -50 ± 5 m at 10 ka in the Cádiz Gulf (Hernández-Molina et al., 1994; Lario, 1996), coinciding with a climatic amelioration between 10 ka and 5.4 ka in this area (Santos et al., 2003).

In the inner shelf (Figure 7, d), the interpretation of high-resolution seismic profiles has permitted to recognize the presence of an elongate sandy barrier that protected an adjacent broad lagoon. Tidal channels of this lagoon had a NW-SE direction and were partially covered by overwash deposits (Lobo et al., 2001). The northeastern part of this lagoon was delimited by aeolian systems (Zazo et al., 2005) and marshes (core PLN; Zazo et al., 1999).

Phase 4 (maximum of the Flandrian transgression -6.5 cal ka BP-)

In the Cádiz Gulf, river mouths were inundated around 6.5 cal ka (Zazo et al., 1994; Borrego et al., 1999; Dabrio et al., 2000). The Doñana National Park was occupied by an open lagoon (Figure 7, e), partially protected in its westernmost part by aeolian units (Zazo et al., 2008). The bottom sediments were constituted by silty sand with abundant remains of marine faunas (core PLN).

After this maximum, the Doñana spit began to grow (Goy et al., 1996), with a progressive limitation of the tidal fluxes. In addition, the Guadiamar River caused the deposition of alluvial terraces at ~6300 yr BP in the northern part of the park (level T2; Salvany et al., 2001).

Phase 5 (6.5-4.6 cal ka BP)

The first part of this phase is characterized by the growth of the Doñana spit, with the progressive emersion of the inner side of this incipient barrier (core AR). The bottom sediments of the adjacent, quiet lagoon were composed of clayey silt (FA-3) with variable bioclastic contents (Figure 7, f).

Between 5100 and 4800 cal BP (Figure 7, g), a tsunami caused the erosion of this spit and the deposition of aeolian sand (FA-6) over the new salt marsh.

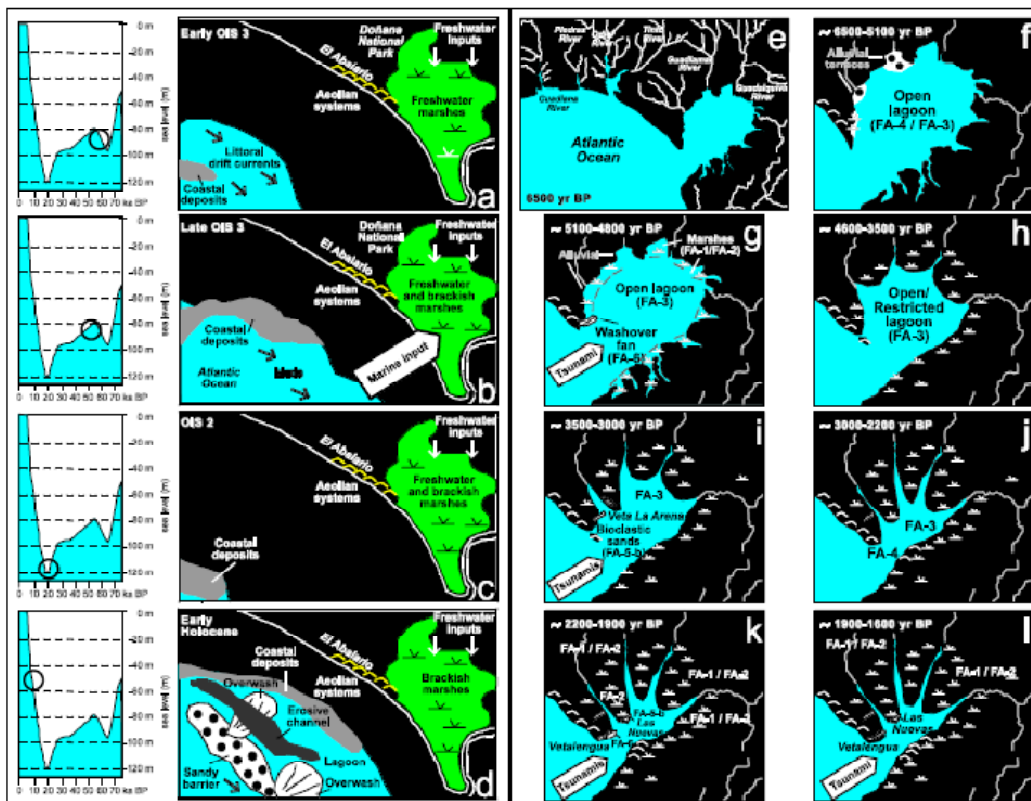


Figure 7. Palaeoenvironmental evolution of the Doñana National Park during the last 65 ka. Left column: Late Pleistocene to Early Holocene sea level changes (modified from Siddall et al, 2003). a-d: southwestern corner modified from Lobo et al. (2001; 2002). Additional data obtained from Goy et al., (1996), Zazo et al. (1999, 2005), Salvany et al. (2001), and Zazo et al. (2008)

Phase 6 (4.6-3.7 cal ka BP)

The central part of the Doñana National Park was still occupied by an open lagoon (cores CR and PLN), whereas the Doñana spit grew toward the southeast. This phase is dominated by the lagoon infilling, with the deposition of phyllosilicate-rich sediments (FA-3) in the lagoon bottom (Figure 7, h).

Phase 7 (3.7-3 cal ka)

This area was subjected to arid conditions during this period (Zazo et al., 2008). One or two tsunami-like events (or very strong storms) caused the erosion of the Doñana spit (Figure 7, i) and the deposition of bioclastic, sandy-clayey silt over the lagoon bottom (core CR). In a latter period, new high-energy events induced the emersion of the very shallow, southwestern areas of the lagoon, with the deposits of FA-5 over intertidal sediments (core BR, CR and PLN).

Phase 8 (3-2.2 cal ka)

During this phase (Figure 7, j), the southwestern part of the Doñana National area remained emerged (cores AR-BR-CR), whereas the central and southern ones were occupied by a very shallow lagoon (core PLN). The continuous growing of the Doñana spit and the progressive infilling induced the creation of new brackish marshes (cores DR-HR; core ML-97, Zazo et al., 1999) or the transition from marine conditions to more restricted scenarios (core CM).

Phase 9 (2.2-1.9 cal ka)

Several tsunamis eroded the Doñana spit in the following phase (Figure 7, k), with the creation of small washover fans constituted by aeolian sediments (core DR and CM) and the accumulation of bioclastic ridges over the lagoon borders (core HR). In addition, the subtidal palaeoenvironments of the central part are covered by bioclastic, silty-sandy sediments (core GR).

Additional sedimentary evidence of these events include erosive surface in the Doñana spit (Rodríguez Ramírez et al., 1995), washover fans near the Gibraltar Strait (Luque et al., 2002), limestone boulders located at +4 to +15 m asl near Lisbon (Scheffers and Kelletat, 2005) or a turbiditic layer in the SW Portuguese Margin (Vizcaino et al., 2006a). These tsunamis may be assimilated to the historical tsunamis that devastated the southwestern Iberian coasts between 218-209 BC and 60 BC (Campos, 1991).

Phase 10 (1.9 cal ka-Present)

The first period of this phase (Figure 7, 1: 1900-1600 cal BP) is characterized by an increasing infilling of the lagoon (cores FR, GR and CM), with a progressive transition toward intertidal-supratidal conditions. This tendency was interrupted by a new introduction of marine sediments and, to a lesser extent, aeolian sediments in the southern part of the park (core FR and, probably, CM), owing to new high-energy events. Ages of these phenomena coincide with those of a historical tsunami (382 BC; Campos, 1991).

The posterior palaeoenvironmental evolution of the Doñana National Park is marked by the creation of new wetlands with temporary ponds (core GR) and the growing of the Doñana and La Algaida spits, with aeolian sands covering intertidal sediments (core CM).

At present, no evidence of the 1755 Lisbon earthquake-induced tsunamis have been found in this area, although some erosive surfaces located in the southeastermost part of the Doñana spit might be originated by this event. These tsunamis settled washover fans near the Gibraltar Strait, imbricated boulders around Lisbon or abyssal tempestites in the SW Portuguese margin (Luque et al., 2001; Scheffers and Kelletat, 2005; Whelan and Kelletat, 2005; Vizcaino et al., 2006b)

6. CONCLUSIONS

A Late Pleistocene to Holocene evolution of the Doñana National Park has been proposed, based on the multidisciplinary analysis (texture, colour, geomorphology, paleontology, mineralogy, dating) of sediments present in two drill cores and seven short cores. This study permits to delimitate the geological features of five sedimentary facies deposited in distinctive palaeoenvironments (freshwater and brackish marshes, open lagoon, external lagoon and sandy spit) and a sixth, heterogeneous facies with a tsunamigenic origin.

Ten phases have been distinguished since OIS 3, with a general scenario of progressive lagoon infilling conditioned temporary by sea level changes and high-energy events. These events caused the deposition of washover fans and bioclastic ridges over previous marshes or the lagoon bottom. This geological scenario was compared with climatic oscillations and sea level changes.

ACKNOWLEDGMENTS

This work was funded by two Spanish DGYCIT Projects (CTM2006-06722 and CGL2006-01412) and three Research Groups of the Andalusia Board (RNM-002, RNM-238 and RNM-293). It is a contribution to IGCP-495 and 526.

REFERENCES

- [1] Babu, N., Suresh Babu, D. S. & Mohan Das, P. N. (2007). Impact of tsunamis on texture and mineralogy of a major placer deposit in southwest coast of India. *Env. Geol.*, *52*, 71-80.
- [2] Barahona, E. (1974). Arcillas de ladrillería de la provincia de Granada: *evaluación de algunos ensayos de materias primas*. Ph.D. Thesis, Granada University, Granada.
- [3] Behre, K. E. (1989). Biostratigraphy of the last glacial period in Europe. *Quat. Sci. Rev.*, *8*, 25-44.
- [4] Borrego, J., Morales, J. A. & Pendón, J. G. (1993). Elementos morfodinámicos responsables de la evolución reciente del estuario bajo del río Guadiana (Huelva). *Geogaceta*, *11*, 86-89.
- [5] Borrego, J., Ruiz, F., González-Regalado, M. L., Pendón, J. G. & Morales, J. A. (1999). The Holocene transgression into the estuarine central basin of the Odiel River mouth (Cádiz Gulf, SW Spain): lithology and faunal assemblages. *Quat. Sci. Rev.*, *18*, 769-788.
- [6] Borrego, J., López González, N. & Carro, B. (2004). Geochemical signature as palaeoenvironmental markers in Holocene sediments of the Tinto River estuary (Southwestern Spain). *Estuar. Coast. Shelf Sci.*, *61*, 631-641.
- [7] Bryant, E. A. (2001). *Natural Hazards*. Cambridge University Press, Hong Kong.
- [8] Bryant, E. A., Young, R. W. & Price, D. M. (1992). Evidence of tsunami sedimentation on the southeastern coast of Australia. *J. Geol.*, *100*, 753-765.
- [9] Campos, M. L. (1991). Tsunami hazard on the Spanish coasts of the Iberian Peninsula. *Sci. Tsunami Haz.*, *9*, 83-90.
- [10] Carbonel, P. & Pujos, M. (1982). Les variations architecturales des microfaunes du lac du Tunis: relations avec l'environnement. In : P. Lasserre, & H. Postma, (Ed.), Coastal lagoons. Proceedings of the International Symposium on Coastal Lagoons, Bordeaux, France. *Oceanologica Acta*, *5*, 79-85.
- [11] Carretero, M. I., Ruiz, F., Rodríguez Ramírez, A., Cáceres, L., Rodríguez Vidal, J. & González-Regalado, M. L. (2002). The use of clay minerals and microfossils in palaeoenvironmental reconstructions: the Holocene littoral strand of Las Nuevas (Doñana National Park, SW Spain). *Clay Min.*, *37*, 93-103.
- [12] Chamley, H. (1989). *Clay Sedimentology*. Springer Verlag, Berlin.
- [13] Clague, J. J., Bobrowsky, P. T. & Hutchinson, I. (2000). A review of geological records of large tsunamis at Vancouver Island, British Columbia. *Quat. Sci. Rev.*, *19*, 849-863.
- [14] Cisternas, M., Arwater, B. F., Torrejon, F., Hawaii, Y., Machuca, G., Lagos, M., Eipert, A., Youlton, C., Salgado, I., Kamataki, T., Shishikura, M., Rajendran, C. P., Malik, J. K., Rizal, Y. & Husni, M. (2005). Predecessors to the giant 1960 Chile earthquake. *Nature*, *437*, 404-407.
- [15] Costa, P., Leroy, S., Kershaw, S. & Dinis, J. (2004). Detecting store and tsunami deposits in coastal lagoons. Preliminary results from Lagoa de Óbidos (Portugal). Abstracts First Joint Meeting of IGCP 490 and ICSU Environmental catastrophes in Mauritania, *the desert and the coast*, Atar, Mauritania.

- [16] Dabrio, C. J., Zazo, C., Lario, J., Goy, J. L., Sierro, F. J., Borja, F., González, J. A. & Flores, J. A. (2000). Depositional history of estuarine infill during the last postglacial transgression (Gulf of Cadiz, southern Spain). *Mar. Geol.*, 162, 381-404.
- [17] Dawson, A. & Smith, D. (2000). The sedimentology of Middle Holocene tsunami facies in northern Sutherland, Scotland, UK. *Mar. Geol.*, 170, 69-79.
- [18] Dawson, A. G. & Steward, I. (2007). Tsunami deposits in the geological record. *Sed. Geol.*, 200, 166-183.
- [19] Dillon, W. R. & Goldstein, M. (1984). *Multivariate Analysis and Applications*. Wiley, New York.
- [20] Duplessy, J. C., Shackleton, N. J., Fairbanks, R. G., Labeyrie, L., Oppo, D. & Kallel, N. (1988). Deepwater source variations during the last climatic cycle and their impact on the global deep circulation. *Palaeoceanography*, 3, 343-360.
- [21] Flor, G. (1990). Tipología de dunas eólicas. Procesos de erosión, sedimentación costera y evolución litoral de la provincia de Huelva (Golfo de Cádiz occidental, Sur de España). *Est. Geol.*, 46, 99-109.
- [22] Galbis, R. J. (1932). Catálogo sísmico de la zona comprendida entre los meridianos 58E y 208W de Greenwich y los paralelos 45° y 25° N. Dirección General del Instituto Geográfico, *Catastral y de Estadística*, Madrid.
- [23] González-Regalado, M. L., Ruiz, F., Baceta, J. I., Pendón, J. G., Abad, M., Hernández-Molina, F. J., Somoza, L. y. & Díaz del Río, V. (2000). Foraminíferos bentónicos actuales de la plataforma continental del norte del Golfo de Cádiz. *Geogaceta*, 29, 75-79.
- [24] Goy, J. L., Zazo, C., Dabrio, C. J., Lario, J., Borja, F., Sierro, F. J. & Flores, J. A. (1996). Global and regional factors controlling changes of coastlines in southern Iberia (Spain) during the Holocene. *Quat. Sci. Rev.*, 15, 773-780.
- [25] Gutiérrez-Mas, J. M., López-Galindo, A. & López-Aguayo, F. (1997). Clay minerals in recent sediments of the continental shelf and the Bay of Cádiz (SW Spain). *Clay Min.*, 32, 507-515.
- [26] Harter, S. K. & Mitsch, W. J. (2003). Patterns of short-term sedimentation in a freshwater created marsh. *J. Environm. Qual.*, 32, 325-334.
- [27] Hernández-Molina, F. J., Somoza, L., Rey, J. & Pomar, L. (1994). Late Pleistocene-Holocene sediments on the Spanish continental shelves: model for very high resolution sequence stratigraphy. *Mar. Geol.*, 120, 129-174.
- [28] Hoge, B. E. (1994). The response of wetlands to sea-level rise: *Ecological, paleoecologic, and taphonomic models*. PhD. Thesis, Rice University, USA.
- [29] Hori, K., Kuzumoto, R., Hirouchi, D., Umitsu, M., Janjirawuttikul, N. & Patanakanog, B. (2007). Horizontal and vertical variation of 2004 Indian tsunami deposits. An example of two transects along the western coast of Thailand. *Mar. Geol.* (239). 163-172.
- [30] Lario, J. (1996). *Último y Presente Interglacial en el área de conexión Atlántico-Mediterráneo: variaciones del nivel del mar, paleoclima y paleoambientes*. Ph. D. Thesis, Universidad Complutense de Madrid, Madrid.
- [31] Lario, J., Zazo, C., Dabrio, C. J., Somoza, L., Goy, J. L., Bardají, T. & Silva, P. G. (1995). Record of Holocene sediment input on spit bards and deltas of south Spain. *J. Coast. Res.*, Special Issue, 17 (*Holocene Cycles: Climate, Sea Levels, and Sedimentation*), 241-245.

- [32] Lario, J., Zazo, C., Goy, J. L., Dabrio, C. J., Borja, F., Silva, P. G., Sierro, F. J., González, A., Soler, V. & Yll, E. (2002). Changes in sedimentation trends in SW Iberia Holocene estuaries (Spain). *Quat. Int.*, 93-94, 171-176.
- [33] Lobo, F. J., Hernández-Molina, F. J., Somoza, L. & Díaz del Río, V. (2001). The sedimentary record of the post-glacial transgression on the Gulf of Cádiz continental shelf. *Mar. Geol.*, 178, 171-195.
- [34] Lobo, F. J., Hernández-Molina, F. J., Somoza, L., Díaz del Río, V. & Dias, J. A. (2002). Stratigraphic evidence of an Upper Pleistocene TST to HST complex on the Cádiz Gulf continental shelf (southwest Iberian Peninsula). *Geo-Mar. Let.*, 22, 95-107.
- [35] Luque, L. (2002). Cambios en los paleoambientes costeros del sur de la Península Ibérica (España) durante el Holoceno. *PhD Thesis*, C.S.I.C.-Universidad Complutense de Madrid.
- [36] Luque, L., Lario, J., Zazo, C., Goy, J. L., Dabrio, C. J. & Silva, P. G. (2001). Tsunami deposits as palaeoseismic indicators: examples from the Spanish coast. *Acta Geol. Hispan.* 3-4, 197-211.
- [37] Luque, L., Lario, J., Civis, J., Silva, P. G., Zazo, C., Goy, J. L. & Dabrio, C. J. (2002). Sedimentary record of a tsunami during Roman times, Bay of Cadiz, Spain. *J. Quat. Sci.*, 17, 623-631.
- [38] Mackie, E. A. V., Lloyd, J. M., Leng, M. J., Bentley, M. J. & Arrowsmith, C. (2007). Assessment of $\delta^{13}\text{C}$ and C/N ratios in bulk organic matter as palaeosalinity indicators in Holocene and Lateglacial isolation basin sediments, northwest Scotlan. *J. Quat. Sci.*, 22, 579-591.
- [39] Marocco, R., Melis, R., Montenegro, M. E., Pugliese, N., Vio, E. & Lenardon, G. (1996). Holocene evolution of the Caorle barrier lagoon (northern Adriatic Sea, Italy). *Riv. Ital. Paleontol. Stratigr.*, 102, 385-396.
- [40] Menanteau, L. (1979). *Les Marismas du Guadalquivir*. Exemple de transformation d'un paysage alluvial au cours du Quaternaire récent. Thèse 3er cycle, Université Paris-Sorbonne.
- [41] Montenegro, M. E. & Pugliese, N. (1996). Autoecological remarks on the ostracod distribution in the Marano and Grado Lagoons (Northern Adriatic Sea, Italy). *Boll. Soc. Paleontol. Ital.*, 3, 123-132.
- [42] Pérez Quintero, J. C. (1989). Introducción a los Moluscos onubenses, I: Faunística. *Junta de Andalucía*, Spain.
- [43] Pozo, M., Ruiz, F., Carretero, M. I., Rodríguez Vidal, J., Cáceres, L. M. & Abad, M. (in press). Mineralogical assemblages, geochemistry and fossil associations of Pleistocene-Holocene siliciclastic deposits from the southwestern Doñana National Park (SW Spain): a palaeoenvironmental approach. *Sedimentary Geology*.
- [44] Reichert, K. (2001). Paleoseismological advances in the Granada Basin (Betic Cordilleras, southern Spain). *Acta Geol. Hispan.*, 36, 267-281.
- [45] Rodríguez Ramírez, A., Siljeström, P., Clemente, L., Rodríguez Vidal, J. & Moreno, A. (1995). Caracterización de las pautas geomorfológicas de la flecha litoral de Doñana. *Rev. Teled.*, 5, 28-32.
- [46] Ruiz, F., González-Regalado, M. L., Serrano, L. & Toja, J. (1996). Los ostrácodos de las lagunas temporales del Parque Nacional de Doñana. *Aestuaría*, 4, 125-140.

- [47] Ruiz, F., González-Regalado, M. L. & Muñoz, J. M. (1997). Multivariate analysis applied to total and living fauna: seasonal ecology of recent benthic ostracoda off the North Cadiz Gulf Coast (SW Spain). *Mar. Micropal.*, 31, 183-203.
- [48] Ruiz, F., González-Regalado, M. L., Baceta, J. I., Menegazzo-Vitturi, L., Pistolato, M., Rampazzo, G. y. & Molinaroli, E. (2000). Los ostrácodos actuales de la laguna de Venecia (NE de Italia). *Geobios*, 33, 447-454.
- [49] Ruiz, F., Rodríguez-Ramírez, A., Cáceres, L. M., Rodríguez Vidal, J., Carretero, M. I., Clemente, L., Muñoz, J. M., Yañez, C. & Abad, M. (2004). Late Holocene evolution of the southwestern Doñana National Park (Guadalquivir Estuary, SW Spain): a multivariate approach. *Palaeogeog., Palaeoclimatol., Palaeoecol.*, 204, 47-64.
- [50] Ruiz, F., Rodríguez-Ramírez, A., Cáceres, L. M., Rodríguez Vidal, J., Carretero, M. I., Abad, M., Olías, M. & Pozo, M. (2005a). Evidence of high-energy events in the geological record: Mid-Holocene evolution of the southwestern Doñana National park (SW Spain). *Palaeogeog., Palaeoclimatol., Palaeoecol.*, 229, 212-229.
- [51] Ruiz, F., Rodríguez-Ramírez, A., Cáceres, L. M., Rodríguez Vidal, J., Carretero, M. I., Abad, M., Olías, M. & Pozo, M. (2005b). Eventos de alta energía durante el Holoceno Medio y reciente en el Parque Nacional de Doñana (SO de España). *VI Reunión de Cuaternario Ibérico*. Gibraltar, UK.
- [52] Ruiz, F., Abad, M., Galán, E., González, I., Aguilá, I., Olías, M., Gómez Ariza, J. L. & Cantano, M. (2006a). The present environmental scenario of El Melah Lagoon (NE Tunisia) and its evolution to a future sabkha. *J. African Earth Sci.*, 44, 289-302.
- [53] Ruiz, F., Abad, M., Olías, M., Galán, E., González, I., Aguilá, E., Hamoumi, N., Pulido, I. & Cantano, M. (2006b). The present environmental scenario of the Nador Lagoon (Morocco). *Env. Res.*, 102, 215-229.
- [54] Salvany, J. M., Medialvilla, C., Mantecón, R. & Manzano, M. (2001). Geología del Valle del Guadiamar y áreas colindantes. *Bol. Geol. y Min. spec.* vol., 57-68.
- [55] Samir, A. M. (2000). The response of benthic foraminifera and ostracods to various pollution sources: a study from two lagoons in Egypt. *J. Foram. Res.*, 30, 83-98.
- [56] Santos, A., Sousa, A., Fernández, R. & García, P. (2006). Aquatic macrophytes in Doñana protected area (SW Spain): an overview. *Limnetica*, 25, 71-80.
- [57] Santos, L., Sánchez-Goñi, M. F., Freitas, M. C. & Andrade, C. (2003). Climatic and environmental changes in the Santo André coastal area (SW Portugal) during the last 15,000 years. In: M. B., Ruiz Zapata, M., Dorado, A., Valdeolmillos, M. A., Gil, T., Bardají, I., Bustamante, & I. Martínez, (Eds.), Quaternary climatic changes and environmental crises in the Mediterranean region. *Alcalá de Henares*, 175-179.
- [58] Scheffers, F. & Kelletat, D. (2005). Boulder deposits on the southern Spanish Atlantic coast: possible evidence for the 1755 AD Lisbon Tsunami. *Sci. Tsunami Haz.*, 23, 25-38.
- [59] Schultz L. G. (1964). Quantitative interpretation of mineral composition from X-ray and chemical data for the Pierre Shale. *US Geol. Survey, Prof. Paper*, 391C.
- [60] Seber, G. A. F. (1984). *Multivariate Observations*. Wiley, New York.
- [61] Selby, K. A. & Smith, D. E. (2007). Late Devensian and Holocene sea-level changes on the Isle of Skye, Scotland, UK. *J. Quat. Sci.*, 22, 119-139.
- [62] Serrano, L. & Toja, J. (1995). Limnological description of four temporary ponds in the Doñana National Park (SW, Spain). *Arch. Hydrobiol.*, 133, 497-516.

- [63] Siddall, M., Rohling, E. J., Almogi-Lavin, A., Hemleben, Ch., Meischner, D., Schmelzer, I. & Smeed, D. A. (2003). Sea-level fluctuations during the last glacial cycle. *Nature*, 423, 853-858.
- [64] Singarasubramanian, S. R., Mukesh, M. V., Manoharan, K., Murugan, S., Bakkiaraj, D. Meter, A. J. & Seralathan, P. (2006). Sediment characteristics of the M-9 tsunami event between Rameswaram and Thoothukudi, Gula of Mannar, southeast coast of India. *Sci. Tsunami Haz.*, 25, 160-172.
- [65] Smith, G. I. (1997). Late Quaternary climates and limnology of the Lake Winnebago, Wisconsin, based on ostracodes. *J. Paleolimnol.*, 18, 249-260.
- [66] Soares, A. M. M. (2008). Radiocarbon dating of marine samples from Gulf of Cádiz. Abstracts Annual Conference IGCP 495, *Faro*, Portugal, 6-7.
- [67] Soares, A. M. M. & Dias, J. M. A. (2006a). Coastal upwelling and radiocarbon evidence for temporal fluctuations in ocean reservoir effect off Portugal during the Holocene. *Radiocarbon*, 48, 45-60.
- [68] Soares, A. M. M. & Dias, J. M. A. (2006b). Once upon a time... the Azores Front penetrated into the Gulf of Cádiz. *Abstracts 5th Symposium on the Iberian Atlantic Margin*, 3.
- [69] Spanish Environmental Ministry, (2005). Proyecto de restauración hidroecológica de la marisma. *Doñana*, 2005.
- [70] Stuiver, M. & Reimer, P. J. (1993). Radiocarbon calibration program. Rev. 4.2. *Radiocarbon*, 35, 215-230.
- [71] Stuiver, M., Reimer, P. J., Bard, E., Beck, J. W., Burr, G. S., Hughen, K. A., Kromer, B., McCormac, F. G., v.d. Plicht, J. & Spurk, M. (1998). INTCAL98 Radiocarbon age calibration 24,000-0 ca BP. *Radiocarbon*, 40, 1041-1083.
- [72] Van Andel, T. H. (2003). Glacial Environments I – The Weichselian Climate in Europe between the end of the OIS-Interglacial and the Last Glacial Maximum. In: T., Van Andel, & W. Davies, (Eds.), *Archaeological Results of the Stage 3, The McDonald Institute for Archaeological Research*. Cambridge, 10-20.
- [73] Van der Kaars, S., Penny, D., Tibby, J., Dam, R. A. C. & Suparan, P. (2001). Late Quaternary palaeoecology, palynology and palaeolimnology of a tropical lowland swamp: Rawa Danau, West-Java, Indonesia. *Palaeogeog., Palaeoclimatol., Palaeoecol.*, 171, 185-212.
- [74] Vanney, J. R. (1970). *L'hydrologie du Bas Guadalquivir*. Ed. CSIC-Consejo Superior de Investigaciones Científicas-. Madrid.
- [75] Vilanova, I., Prieto, A. R. & Espinosa, M. (2006). Palaeoenvironmental evolution and sea-level fluctuations along the southeastern Pampa grasslands coast of Argentina during the Holocene. *J. Quat. Sci.*, 21, 227-242.
- [76] Vizcaino, A., Gràcia, E., Escutia, C., Asioli, A., García-Orellana, J., Lebreiro, S., Cacho, I., Thouveny, N., Larrasoana, J. C., Díez, S. & Dañobeitia, J. J. (2006a). Characterizing Holocene Paleoseismic Record in the SW Portuguese Margin. *Geophys. Res. Abstracts*, 8, 08469.
- [77] Vizcaino, A. Gràcia, E., Pallàs, R., Garcia-Orellana, J., Escutia, C., Casas, D., Willmott, V., Díez, S., Asioli, A. & Dañobeitia, J. (2006b). Sedimentology, physical properties and ages of mass-transported deposits to the Marqués de Pombal, Fault, Southwest Portuguese Margin. *Norv. J. Geol.*, 86, 177-186.

- [78] Wagner, B., Bennike, O., Klug, M. & Cremer, H. (2007). First indication of Storegga tsunami deposits from East Greenland. *J. Quat. Sci.*, 22, 321-325.
- [79] Whelan, F. & Kelletat, D. (2005). Boulder deposits on the Southern Spanish Atlantic Coast: Possible evidence for the 1755 AD Lisbon tsunami. *Sci. Tsunami Haz.*, 23, 25-38.
- [80] Whittecar, G. R., Megonigal, J. P. & Darke, A. K. (2001). Sedimentation patterns within tidal fresh-water marshes, Mattaponi River, Virginia. *GSA Annual Meeting*, Boston, Session 180, booth 69.
- [81] Yll, R., Zazo, C., Goy, J. L., Pérez-Obiol, R., Pantaleón-Cano, J., Civis, J., Dabrio, C., González, A., Borja, F., Soler, V., Lario, J., Luque, L., Sierro, F. J., González-Hernández, F. M., Lezine, A. M., Deneffe, M. & Roure, J. M. (2003). Quaternary palaeoenvironmental changes in south Spain. In: M. B., Ruiz Zapata, M., Dorado, A., Valdeolmillos, M. A., Gil, T., Bardají, I. Bustamante, & I. Martínez, (Eds.), Quaternary climatic changes and environmental crises in the Mediterranean region. *Alcalá de Henares*, 201-213.
- [82] Yokoyama, Y., Tezer, M. E. & Lambeck, K. (2001). Coupled climate and sea-level changes deduced from Huon Peninsula cora terraces of the last ice age. *Earth Plan. Sci. Let.*, 193, 579-587.
- [83] Zazo, C., Goy, J. L., Hillaire-Marcel, C., Dabrio, C. J., Belloumini, G., Improta, S., Lario, J., Bardají, T. & Silva, P. G. (1994). Holocene sequence of sea-level fluctuations in relation to climatic trends in the Atlantic-Mediterranean linkage coast. *J. Coast. Res.*, 10, 933-945.
- [84] Zazo, C., Dabrio, C. J., González, A., Sierro, F. J., Yll, E. I., Goy, J. L., Luque, L., Pantaleón-Cano, J., Soler, V., Roure, J. M., Hoyos, M. & Borja, F. (1999). The record of the later glacial and interglacial periods in the Guadalquivir marshlands (Mari López drilling, S. W. Spain). *Geogaceta*, 26, 119-122.
- [85] Zazo, C., Mercier, N., Silva, P. G., Dabrio, C. J., Goy, J. L., Roquero, E., Soler, V., Borja, F., Lario, J., Polo, D. & Luque, L. (2005). Landscape evolution and geodynamic controls in the Gulf of Cádiz (Huelva coast, Spain) during the Late Quaternary. *Geomorphology*, 68, 269-290.
- [86] Zazo, C., Dabrio, C. J., Goy, J. L., Lario, J., Cabero, A., Silva, P. G., Bardají, T., Mercier, N., Borja, F. & Roquero, E. (2008). The coastal archives of the last 15 ka in the Atlantic-Mediterranean Spanish linkage area: Sea level and climate changes. *Quat. Int.*, 181, 72-87.

Figure 3 to 7 Missing